PRDM1 silences stem cell-related genes and inhibits proliferation of human colon tumor organoids

Changlong Liu[a], Carolyn E. Banister[a], Charles C. Weige[a], Diego Altomare[a], Joseph H. Richardson[b], Carlo M. Contreras[b], and Phillip J. Buckhaults[a,1]

[a]Department of Drug Discovery and Biomedical Sciences, College of Pharmacy, University of South Carolina, Columbia, SC 29208; and [b]Division of Surgical Oncology, Department of Surgery, The University of Alabama at Birmingham, Birmingham, AL 35233

Edited by Kenneth W. Kinzler, The Sidney Kimmel Comprehensive Cancer Center at Johns Hopkins University, Baltimore, MD, and approved April 27, 2018 (received for review February 21, 2018)

PRDM1 is a tumor suppressor that plays an important role in B and T cell lymphomas. Our previous studies demonstrated that PRDM1β is a p53-response gene in human colorectal cancer cells. However, the function of PRDM1β in colorectal cancer cells and colon tumor organoids is not clear. Here we show that PRDM1β is a p53-response gene in human colon organoids and that low PRDM1 expression predicts poor survival in colon cancer patients. We engineered PRDM1 knockouts and overexpression clones in RKO cells and characterized the PRDM1-dependent transcript landscapes, revealing that both the α and β transcript isoforms repress MYC-response genes and stem cell-related genes. Finally, we show that forced expression of PRDM1 in human colon cancer organoids prevents the formation and growth of colon tumor organoids in vitro. These results suggest that p53 may exert tumor-suppressive effects in part through a PRDM1-dependent silencing of stem cell genes, depleting the size of the normal intestinal stem cell compartment in response to DNA damage.

TP53 | PRDM1 | colorectal cancer | organoids | CRISPR

PRDM1 is a positive regulatory domain zinc finger protein, which is also known as "B lymphocyte-induced maturation protein" (Blimp-1). It was first identified as a protein that binds to and represses expression from the IFN-β promoter (1). It is a master regulator of the differentiation of plasma cells from B cells, driving plasma cell differentiation (2). PRDM1 plays critical roles in the differentiation and development of many other types of cells in mouse and in other model organisms (3–7). PRDM1 induces B cell maturation by affecting genes that are critical for mature B cell identity and cellular proliferation (8–10). In T cells, PRDM1 is expressed in both memory and effector cell types, and it regulates the homeostasis of these two populations (11, 12). PRDM1 is induced by IL-2, which is itself regulated by PRDM1 through the binding of PRDM1 to the IL-2 promoter. This auto feedback forms a regulation loop in T cells (13, 14). In the early developing mammalian embryo, PRDM1 controls global epigenetic changes that are required for specification of the primordial germ cells (15–17). In primordial germ cells, PRDM1 associates with PRMT5, an arginine-specific histone methyl transferase, and induces the dimethylation of arginine 3 of the histone H2A and H4 tails. The PRDM1 and PRMT5 complex is implicated in repressing genes associated with a somatic cell program, thus maintaining the primordial germ cells in an undifferentiated state (18).

PRDM1 is a transcriptional repressor with mechanisms that vary in a context-dependent manner. PRDM1 has DNA-binding activity and the ability to recruit diverse chromatin-modifying proteins, such as G9a, HDAC1, HDAC2, and the transcriptional corepressor Groucho, generating regulatory complexes that can silence specific genes during cell differentiation (19–21). PRDM1 recruits the G9a methyltransferase through the first two zinc fingers, thus leading to H3K9 methylation and transcriptional silencing (20). PRDM1 target genes have been reported in several tissues. In plasma cells PRDM1 represses the expression of genes encoding c-Myc, Spi-B, Id3, and Pax-5 (8). In human and mouse cells PRDM1 target genes include *IFN-β*, *KLF4*, *IL-2*, *c-Fos*, *Dusp16*, and *TP53* (1, 7, 13, 20, 22).

PRDM1 interacts with the p53 tumor-suppressor pathway, and its ability to repress genes indicates it may have an important role as a tumor suppressor (23). In HCT116 cells, PRDM1 regulates cell growth through the repression of p53 transcription, and p53 is able to activate PRDM1 expression by binding to an alternative promoter (22). Our previous study has shown that PRDM1 is activated by specific polymorphic variants of p53 in RKO colon cancer cells (24). Also a recent study showed that PRDM1can inhibit SW620 colon cancer cell proliferation by inhibiting c-Myc (25). The mechanisms by which PRDM1 acts on human colon cells is incompletely understood and may lead to insights relevant to colon cancer and normal intestinal stem cell maintenance. In this study, we knocked out and overexpressed PRDM1 in RKO colon cancer cells and in colon cancer organoids to address the roles of PRDM1 and its target gene landscape in colon cancer cell proliferation. We show that PRDM1 activates and represses a large number of target genes related to proliferation and differentiation and that it powerfully inhibits clonogenic survival of primary colon tumor organoids.

Results

PRDM1 Is a p53-Responsive Gene in Normal Colon Organoids and Is Correlated with Disease-Free Survival in Colon Cancers. The *PRDM1* gene encodes a long, 5,164-bp transcript (PRDM1α) and a

Significance

Our previous studies demonstrated that PRDM1β is activated by p53 accumulation in human colorectal cancer cells. However, the function of PRDM1β in colorectal cancer cells and colon tumor organoids is not clear. Here we show that PRDM1β is a p53-response gene in human colon organoids and that low PRDM1 expression predicts poor survival in colon cancer patients. Also, PRDM1α and PRDM1β proteins repress a largely overlapping suite of genes, many of which are stem cell-related genes. Moreover, we show that forced expression of PRDM1β prevents the proliferation of colon tumor organoids. This work provides support for a role of PRDM1β in regulating normal colon stem cell proliferation.

Author contributions: C.L. and P.J.B. designed research; C.L., C.E.B., C.C.W., D.A., J.H.R., and C.M.C. performed research; J.H.R. and C.M.C. contributed new reagents/analytic tools; C.L. and P.J.B. analyzed data; and C.L. and P.J.B. wrote the paper.

The authors declare no conflict of interest.

This article is a PNAS Direct Submission.

Data deposition: The data reported in this paper have been deposited in the Gene Expression Omnibus (GEO) database, https://www.ncbi.nlm.nih.gov/geo (accession no. GSE101668).

[1]To whom correspondence should be addressed. Email: phillip.buckhaults@gmail.com.

This article contains supporting information online at www.pnas.org/lookup/suppl/doi:10.1073/pnas.1802902115/-/DCSupplemental.

Published online May 14, 2018.

shorter 4,675-bp transcript (PRDM1β) (Fig. 1*A*). The two transcripts differ in transcriptional start sites and in the lengths of their coding sequences, with PRDM1β encoding a 727-aa protein that is 102 aa shorter than the larger protein encoded by PRDM1α. The short-transcript isoform contains a unique 5′ UTR, starting from a transcriptional start site located within intron 3. The relative activities of these two isoforms are not understood, although some results suggest that PRDM1β encodes an inactive or less active polypeptide (26). Overall the expression of both PRDM1 isoforms is low in most colon cancer cell lines. We confirmed this by examining GSE46549 data (*SI Appendix*, Fig. S1*A*) (27). We and others have previously shown that PRDM1β is activated by p53 (22, 24). To explore PRDM1 regulation in human primary colon cells, we cultured human normal colon organoids named "P08182015" (Table 1) in 3D culture (Fig. 1*B*) (28–30) that contained heterogeneous cell populations, reflecting the in vivo cell-type diversity. We activated the p53 protein (Fig. 1*D*) by treating the organoids with either the MDM2 inhibitor nutlin3a (31) or the DNA-damaging agent etoposide. Both *GDF15*, a known p53-response gene (24), and PRDM1β, but not PRDM1α (*SI Appendix*, Fig. S1*B*), were significantly increased after exposure to nutlin3a or etoposide (Fig. 1 *C* and *D*).

We reasoned that p53 mutation could lead to the reduction of PRDM1 expression in colorectal tumors. To assess this, we analyzed the expression of PRDM1 in 222 colorectal cancer

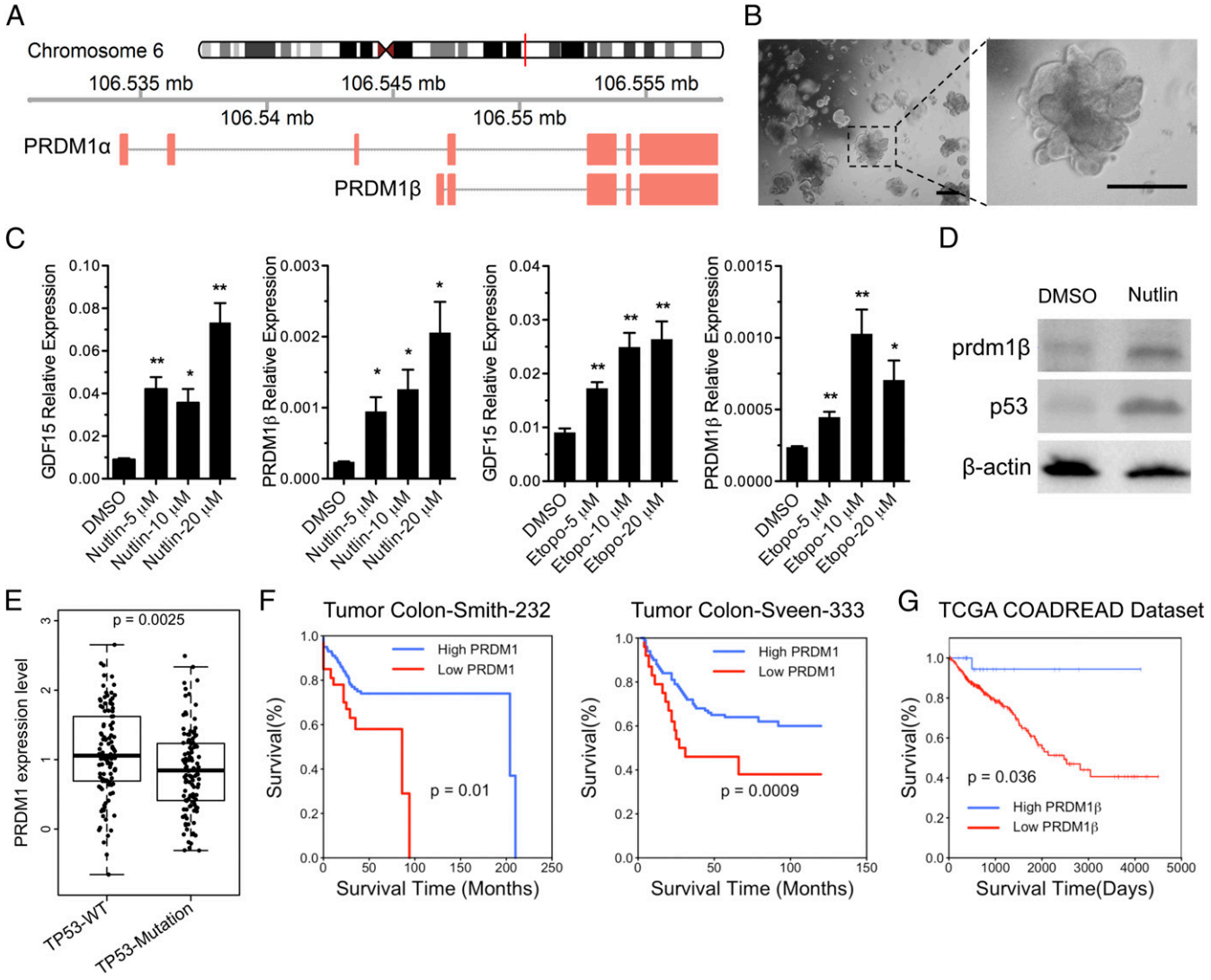

Fig. 1. PRDM1 is a p53-responsive gene in human normal colon organoids and is correlated with disease-free survival in colon cancers. (*A*) Schematic representation of two transcript isoforms (PRDM1α and PRDM1β) derived from the human *PRDM1* gene. (*B*) Morphology of a human normal colon organoid culture in vitro. (Scale bars: 2 mm.) (*C*) Organoids were treated with either nutlin3a or etoposide, and PRDM1β expression was evaluated by qPCR. The GDF15 expression level was determined as control. Data are shown as the mean ± SEM of technical triplicates. $*P < 0.05$, $**P < 0.01$. (*D*) PRDM1β protein and p53 levels were determined by Western blot on normal colon organoids that were treated with nutlin3a for 48 h. (*E*) The boxplot shows PRDM1 expression in colorectal tumors in the context of TP53-WT ($n = 110$) or TP53-Mutation ($n = 112$) from the TCGA database. The *y* axis is log2 scale of expression. Each dot represents one patient. (*F*) The Kaplan–Meier survival plots were obtained using the R2 Genomics Analysis and Visualization Platform (https://hgserver1.amc.nl/cgi-bin/r2/main.cgi) and display the probability of disease-free survival of 209 colon cancer patients: high PRDM1 >212.9, $n = 176$; low PRDM1 <212.9, $n = 33$. (*Left*) and 320 colon cancer patients: high PRDM1 >227.6, $n = 272$; low PRDM1 <227.6, $n = 48$. (*Right*). (*G*) Patient survival and PRDM1β expression information was obtained from Xena Functional Genomics Explorer. The Kaplan–Meier survival plot was generated using R2 Kaplan Meier Scanner and displays the probability of disease-free survival of 357 colon cancer patients (PRDM1β expression range: 0 to ~2.79; high PRDM1 >1.345, $n = 25$; low PRDM1 <1.345, $n = 332$). *P* values on the plots are from the log-rank test for the comparisons of the low and high PRDM1 expression groups.

Table 1. Organoid information used in this study

Name	Patient age, y	Patient gender	Stage	TP53 status	Organoid type
P08182015	57	Female	IV	Wild type	Normal
P10152015	56	Male	IIA	Mutant	Tumor
P07132016	62	Male	IIA	Mutant	Tumor

patients from The Cancer Genome Atlas (TCGA) COAD-READ samples for which both PRDM1 expression and TP53 mutation data were available. PRDM1 expression in TP53 wild-type colorectal tumors is significant higher than found in TP53-mutant colorectal tumors (Fig. 1*E*). These data showed that PRDM1β is a p53-regulated gene in primary human normal colon organoids and colorectal tumors. Next, we examined PRDM1 gene expression in published datasets with clinical outcome information and noted that the loss of PRDM1 expression is correlated with poor survival in B cell lymphoma (*SI Appendix*, Fig. S1*C*) and in colon adenocarcinoma (Fig. 1 *F* and *G*).

Generation and Characterization of PRDM1-KO and PRDM1-Overexpressing RKO Cell Lines. To evaluate the roles of PRDM1 in colon cancer cells, first we generated PRDM1-KO derivatives in RKO colon cancer cells by employing CRISPR/Cas9 technology. We developed a strategy that used two small guide RNAs (sgRNAs) to create a deletion of the intervening segment by inducing two double-strand breaks (DSBs) into genomic DNA (Fig. 2*A*) (32, 33). We designed eight sgRNAs and synthesized them as gBlock fragments containing the U6 promoter and the guide RNA (gRNA) targeting and scaffold sequence (Fig. 2*B*). The Cas9-GFP plasmid (34) and sgRNA pairs were simultaneously introduced into cells and then were subjected to FACS based on GFP (Fig. 2*C*). We tested the abilities of several pairs of sgRNAs to induce PRDM1 genomic deletions large enough to detect by sizing PCR products spanning the deleted regions (*SI Appendix*, Fig. S2*A*). The ability to create a genomic deletion was tested by conventional PCR using primer pairs located outside the sgRNAs' binding region (*SI Appendix*, Table S1). We obtained individual KO clones that knocked out only PRDM1α (sgRNA1–sgRNA2 and sgRNA3–sgRNA4) (*SI Appendix*, Fig. S2*B*), clones that knocked out only PRDM1β (sgRNA5–sgRNA7 and sgRNA6–sgRNA7) (*SI Appendix*, Fig. S2*C*), and clones that knocked out both PRDM1α and PRDM1β (sgRNA1–sgRNA8) (Fig. 2 *D* and *E*). We analyzed 24 randomly selected individual clones potentially knocked out for both PRDM1α and PRDM1β by PCR with primers flanking the disrupted region (Fig. 2*D*, outer primers indicated by red arrows) and noted the presence of at least one allele of an abnormal sized PCR product in 18 samples (75%) (Fig. 2*E*). The absence of both alleles of the intervening deleted region was confirmed by PCR using primers completely contained within the removed region flanking exon 2 (Fig. 2*D*, inner primers indicated by green arrows). Of the 18 clones with at least one disrupted allele, we noted five clones that were completely devoid of exon2 sequences. (Fig. 2*E*, *Lower*). We then randomly selected two clones with disrupted PRDM1α and PRDM1β for further characterization by cell proliferation. PRMD1 disruption had no noticeable effect on RKO cell morphology (Fig. 2*F*) or on cell proliferation as assayed by 5-ethynyl-2′-deoxyuridine (EdU) imaging (Fig. 2*G*). These results demonstrated a robust method to produce genomic deletions using CRISPR/Cas9 technology and that the PRDM1 gene is not necessary for the survival of RKO colon cancer cells in vitro. Then we treated TP53 wild-type RKO, TP53-KO RKO, PRDM1 wild-type RKO, and PRDM1-KO RKO cells with nutlin3a or with DMSO as a control. The result showed that p53 was activated by nutlin3a except in the p53-KO RKO cells, and PRDM1β was activated after nutlin3a treatment in wild-type RKO cells. However, PRDM1β is not activated in p53-KO RKO cells or in PRDM1-KO RKO cells after nutlin3a treatment (*SI Appendix*, Fig. S2*D*).

We next generated PRDM1α- and PRDM1β-overexpressing (OE) derivatives of RKO colon cancer cells. We cloned PRDM1α and PRDM1β cDNA into a lentiviral vector which encodes a GPF marker polypeptide linked to the PRDM1 gene product by the P2A peptide sequence. We also generated a control vector expressing only GFP (Fig. 2*H*). We produced replication-defective viral particles in the 293T packaging line and infected RKO cells at a multiplicity of infection (MOI) of 3.0 to produce pools of PRDM1α-, PRDM1β-, and GFP-OE cells. Three days after infection, we isolated the GFP^+ cells by FACS. The PRDM1α-OE and PRDM1β-OE cells were viable and exhibited morphology similar to that of GFP-OE cells (Fig. 2*I*). PRDM1α-OE and PRDM1β-OE cells showed high levels of PRDM1α and PRDM1β transcript (Fig. 2*J*) and protein expression (Fig. 2*K*).

PRDM1α and PRDM1β Have Similar Response Genes in RKO Cells. The PRDM1 transcript landscape in colon cancer cells is not yet described nor are the relative contributions of the PRDM1α and -β isoforms to PRDM1-response gene expression. To identify the transcriptional differences between PRDM1-KO cells and PRDM1α- and PRDM1β-OE RKO cells, we performed RNA-sequencing (RNA-seq) experiments on the cell lines listed in *SI Appendix*, Fig. S3*A*. We obtained more than 30 million uniquely mapped reads for each sample (*SI Appendix*, Fig. S3*B*), with the two biological replicates of each sample being highly reproducible (*SI Appendix*, Fig. S3*C*). First, we evaluated the global changes in gene expression induced by PRDM1α overexpression and PRDM1β overexpression compared with PRDM1 KO. We found that the set of genes regulated by PRDM1α was highly similar to that regulated by PRDM1β (Fig. 3*A*). We observed 2,820 genes that were significantly different [false discovery rate (FDR) adjusted $P < 0.05$] between PRDM1-KO and either PRDM1α-OE or PRDM1β-OE cells. Surprisingly, over half of these genes (1,625) were significantly different in both the PRDM1α and the PRDM1β isoforms (FDR adjusted $P < 0.05$) (Fig. 3*B*). We identified 925 genes that were up-regulated and 727 genes that were down-regulated by both PRDM1α and PRDM1β (FDR adjusted $P < 0.05$) (Fig. 3*C*). The genes that were repressed by both PRDM1α and PRDM1β included *MYC* and *ID3*, previously reported in B cells (8), and *CDK6* and *JAG1*. Interestingly, we found that members of JUN family—JUN, JUNB, and JUND—were activated by PRDM1. Unsupervised hierarchical cluster analysis shows high concordance between the replicate cell lines for both PRDM1α and PRDM1β expression, as well as in two broad classes of genes, those that are repressed and those that are activated (Fig. 3*D*). These results indicate that PRDM1α and PRDM1β may have a similar function in the regulation of cell biology.

PRDM1 Arrested MYC Transcriptional Programs by Inhibiting *MYC* Gene Expression. To examine the possible biological influences of gene networks regulated by PRDM1 in colon cancer cells, we rank ordered all expressed genes by their expression ratio in PRDM1-OE versus PRDM1-KO cells and performed unbiased

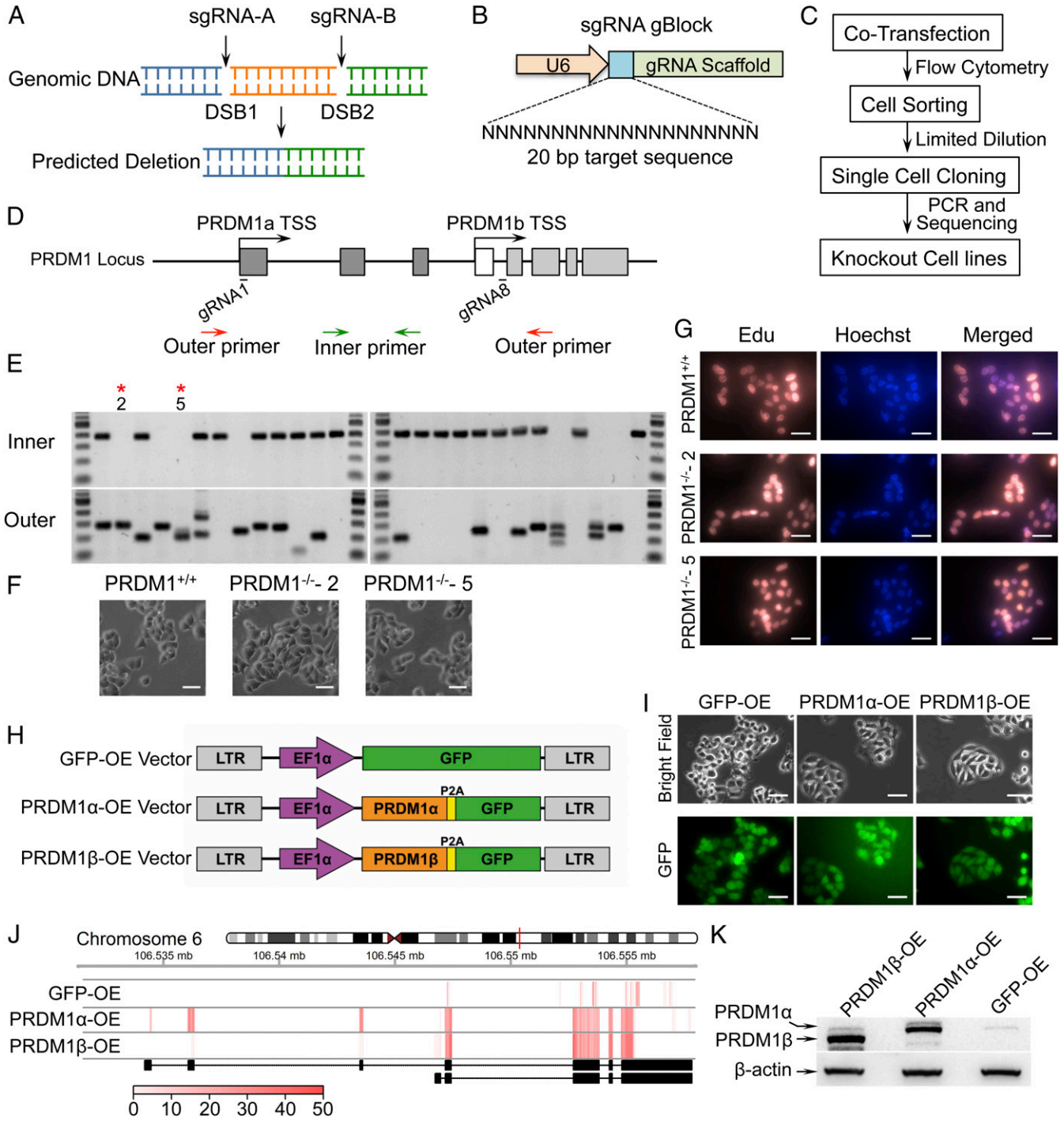

Fig. 2. Generating PRDM1-KO and PRDM1-OE RKO cell lines. (*A*) Schema of the strategy using two sgRNAs and CRISPR/Cas9. Two sgRNAs (sgRNA-A and sgRNA-B) were designed to remove a piece of DNA from the PRDM1 gene. Two DSBs were induced by transient expression of sgRNA-A and sgRNA-B plus CRISPR/Cas9. (*B*) Small synthetic genes (455 bp) encoding sgRNAs were synthesized as gBlocks containing the U6 promoter, the gRNA targeting region, and the scaffold sequence. (*C*) The procedure for generating KO clones. (*D*) Schematic illustration of the *PRDM1* gene locus, sgRNAs, and screening primer locations. About 13 kb of the DNA sequence between gRNA1 and gRNA8 was deleted. (*E*) PCR screening of individual clones. Clones positive for outer and negative for inner PCR products were considered null for both PRDM1 alleles. PRDM1-KO-2 and PRDM1-KO-5 clones are shown. (*F*) Morphology of PRDM1 wild-type RKO cells and PRDM1-KO RKO cells. (Scale bars: 200 μm.) (*G*) Cell proliferation was visualized by the incorporation Edu (orange); the counterstain was Hoechst (blue). (Scale bars: 200 μm.) (*H*) Schematic illustration of lentiviral vectors used for PRDM1 overexpression. The GFP-only vector was constructed as a control. (*I*) Morphology of GFP-only, PRDM1α-OE, and PRDM1β-OE RKO cell lines. (Scale bars: 200 μm.) (*J*) Heatmap of PRDM1 exon expression derived from RNA-seq reads. (*K*) PRDM1α and PRDM1β protein levels were determined by Western blot.

gene set enrichment analysis (GSEA) using the Hallmark dataset from the Molecular Signatures Database (MSigDB) (35). We characterized the transcriptional consequences of PRDM1 in colon cancer cells (Fig. 4*A*). PRDM1 is known to regulate IFN genes, as it was first isolated as a repressor of the IFN-β promoter (1). We observed that IFN-response genes were strongly

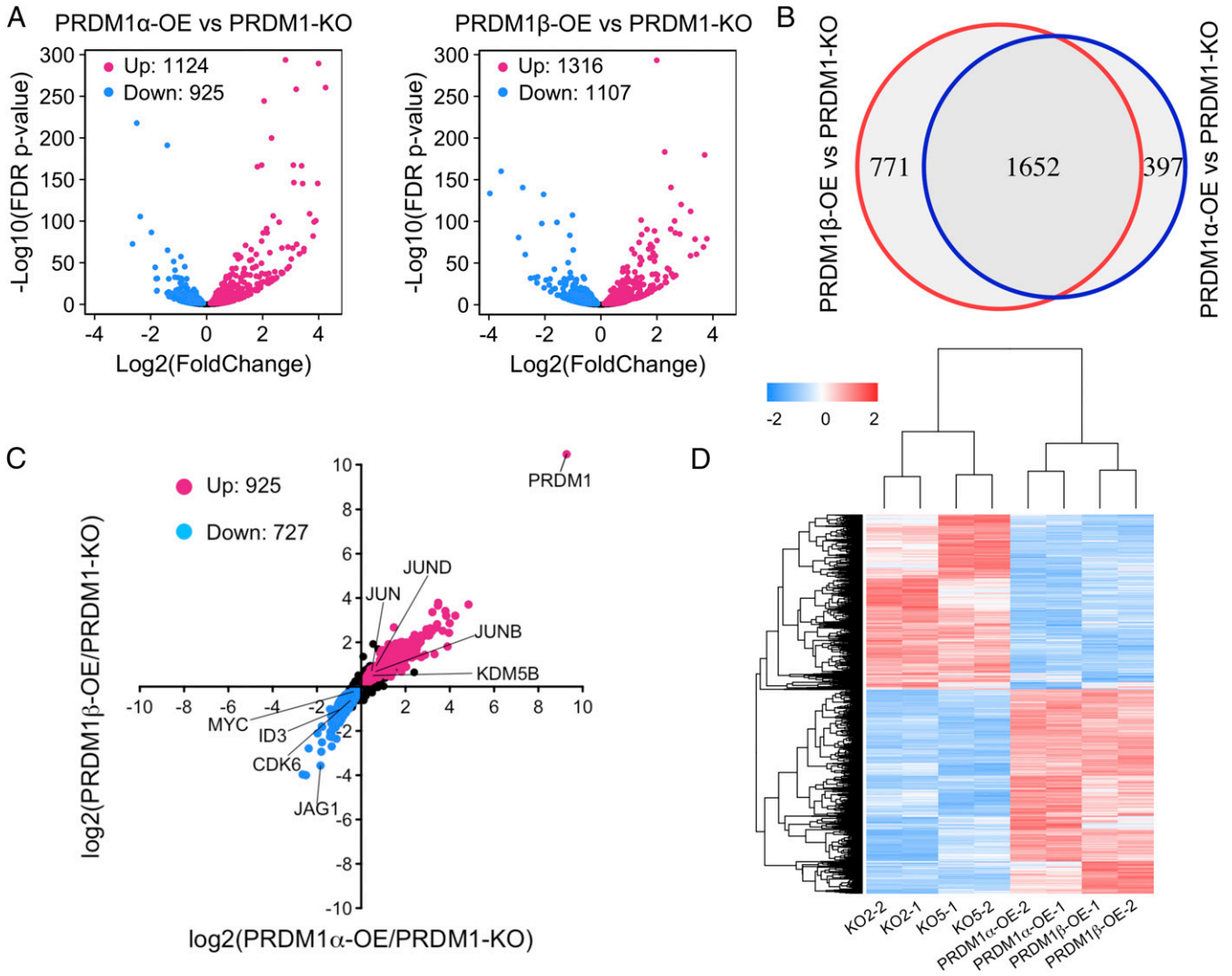

Fig. 3. Global differential gene expression of PRDM1-KO and PRDM1-OE RKO cells. (*A*) Volcano plots comparing differential gene-expression levels between PRDM1-KO and PRDM1α-OE RKO cells and between PRDM1-KO and PRDM1β-OE RKO cells. Red dots show up-regulated genes, and blue dots show genes that are repressed in PRDM1-OE cells compared with PRDM1-KO cells (FDR $P < 0.05$). (*B*) Venn diagrams display the gene set of overlap between PRDM1α- and PRDM1β-regulated genes compared with PRDM1-KO. (*C*) The scatter plot shows 925 genes up-regulated and 727 genes down-regulated by both PRDM1α and PRDM1β. (*D*) Heat map showing common differentially expressed genes in each replicate.

repressed by PRDM1 in RKO colon cancer cells (*SI Appendix*, Fig. S4*A*). PRDM1 was initially described as a master regulator of B cell differentiation, repressing *ID3*, *NFIX*, *PSMB10*, *PSM8*, *SP110*, and *TAPBP* (36). We found that these B cell target genes were also highly repressed by PRDM1 in RKO colon cancer cells (*SI Appendix*, Fig. S4*B*). Among all gene sets in the Hallmark dataset, MYC targets were significantly enriched among the PRDM1 down-regulated genes (Fig. 4*B*). Consistent with previous reports in HCT116 cells (22), we observed that MYC mRNA levels negatively correlated with PRDM1 expression (Fig. 4*C*), which we confirmed in RKO cells by real-time qPCR (Fig. 4*D*) and Western blot (Fig. 4*E*). These results indicate that PRDM1 may inhibit cell proliferation by inhibiting the MYC transcriptional program.

PRDM1 Inhibits Tumor Organoid Formation in 3D Culture. It has been reported that reconstitution of PRDM1 leads to impaired G2/M cell-cycle progression in PRDM1-null NK cell lines (23). We performed GSEA on the entire set from the transcription factor target gene signature from the MSigDB (*SI Appendix*, Fig. S5 *A* and *B*) and tested cell-cycle distributions (*SI Appendix*, Fig. S5 *C–E*). These results suggested that PRDM1 could regulate the cell cycle. Then we tested the proliferation rates of RKO derivatives. PRDM1 engineering had a minimal effect on RKO cell growth (*SI Appendix*, Fig. S5*F*). Therefore we evaluated the function of PRDM1 in human colon tumor organoids grown in 3D culture. To this end, we isolated and established two human colon tumor organoid lines from clinical surgery specimens, which we named "P07132016" and "P10152015" (Table 1). These organoid lines could proliferate for over a year without WNT3a in 3D culture in vitro (*SI Appendix*, Fig. S6 *A* and *B*). We checked PRDM1β expression levels in these organoids and found the expression level of PRDM1β was low in P10152015 and was undetectable in P07132016 (*SI Appendix*, Fig. S6*C*). Because p53 protein activation results in PRDM1β transcript activation, we overexpressed PRDM1β in these human tumor organoids by lentiviral infection (*SI Appendix*, Fig. S6*C*) and collected GFP^+ and GFP^- cells at different time points by cell sorting. We then performed an organoid-forming assay on $PRDM1^+$ and $PRDM1^-$ cells (Fig. 5*A*). We first noted that

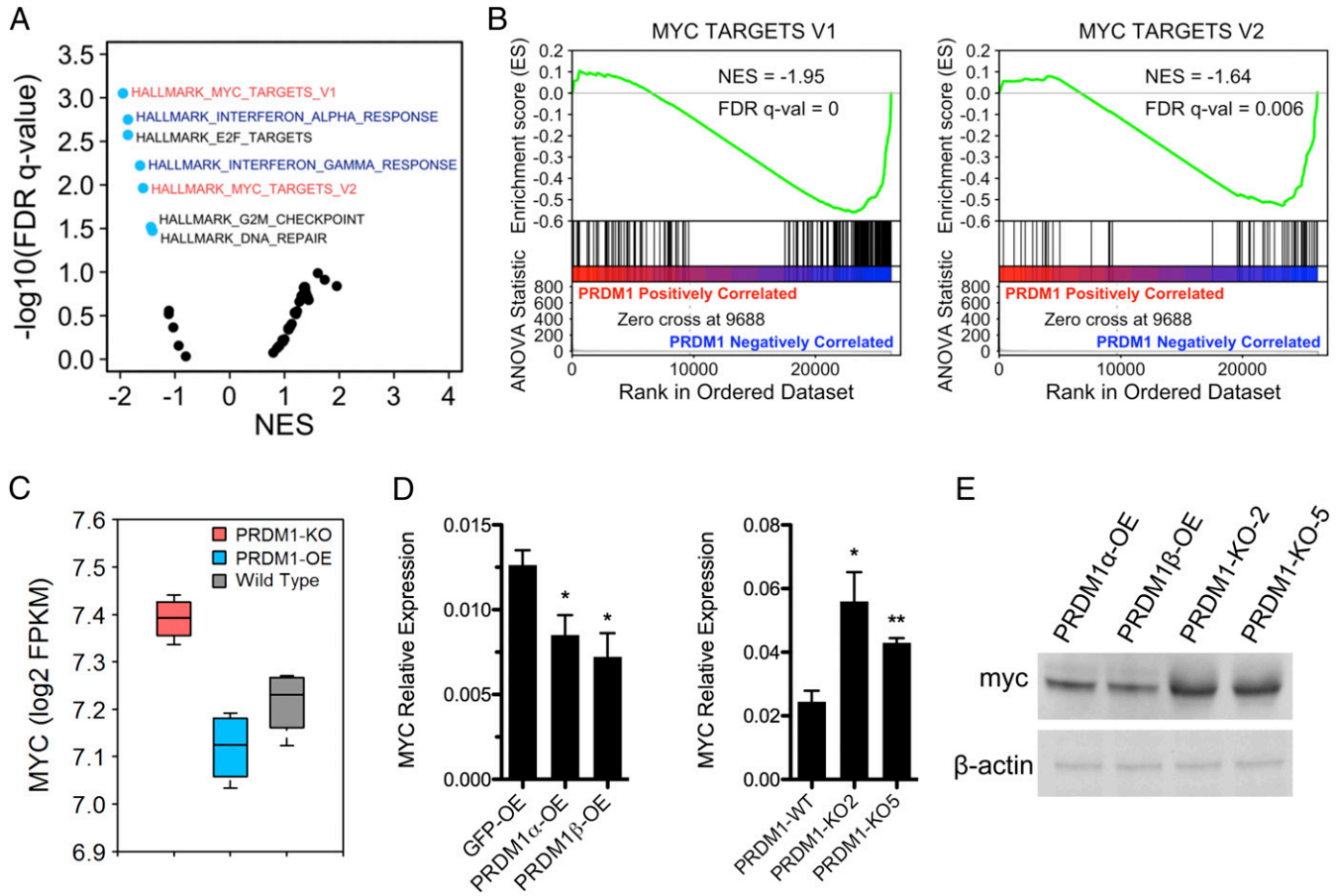

Fig. 4. PRDM1 inhibits MYC and MYC target genes. (*A*) Volcano plot of GSEA of the MSigDB Hallmark database. The FDR versus the normalized enrichment score (NES) for each evaluated gene set is shown. Blue dots are significantly enriched gene sets (FDR adjusted *P* value <0.05). (*B*) GSEA of MYC target genes, rank ordered by ANOVA T statistic. (*C*) Relative expression levels of MYC in RKO cells by RNA-seq. (*D*) mRNA levels determined by qPCR in PRDM1-KO and PRDM1-OE RKO cells. Data are shown as the mean ± SEM of technical triplicates. $*P < 0.05$, $**P < 0.01$. (*E*) Myc protein levels in PRDM1-OE and PRDM1-KO RKO cells were determined by Western blotting.

PRDM1β infection had a dramatic negative impact on cell numbers in both P07132016 (Fig. 5*B*) and P10152015 organoids (Fig. 5*D*). The percentage of PRDM1$^+$ cells dropped from day 2 to day 20 compared with control GFP cells, which increased during the same period (Fig. 5 *C* and *E*). GFP$^+$ and GFP$^-$ cells were obtained from the PRDM1β and control lentivirus infections and were plated to assess organoid-formation abilities. PRDM1-expressing cells proliferated very slowly in P07132016 and formed only very small organoids compared with control cells. However, GFP$^-$ cells from the same transduction proliferated very well and formed regular tumor organoids (Fig. 5 *F* and *G* and *SI Appendix*, Fig. S6*E*). In P10152015 organoids, the PRDM1-expressing cells were viable but did not proliferate or expand into organoids in 3D culture (Fig. 5 *H* and *I* and *SI Appendix*, Fig. S6*E*). We also knocked out PRDM1 in the two organoids P10152015 and P07132016 and performed organoid-forming assays in 3D cultures. The result showed that there was no significant difference between control sgRNA and PRDM1 sgRNA (*SI Appendix*, Fig. S6*F*), probably due to the low level of PRDM1 expressed in both tumor organoids.

Previous studies have shown an embryonic stem cell-like gene-expression signature in breast cancer (37) and in poorly differentiated aggressive human tumors (38). Also, an intestinal stem cell signature could identify colorectal cancer stem cells (39). Therefore we performed GSEA analysis using RNA-seq data in RKO cells on these signatures and found PRDM1 could result in the down-regulation of embryonic stem cell signature and intestinal stem cell signature in colon cancer cells (Fig. 6*A*). These results indicate that forced expression of PRDM1β in colon tumor organoids prevents cancer stem cell proliferation and expansion, possibly through silencing of the stem cell gene-expression network.

Discussion

We have investigated the role of PRDM1 in both RKO colon cancer cells and human colon tumor organoids by PRDM1-KO and PRDM1 overexpression. We developed a strategy of using two sgRNAs to efficiently create a deletion of the intervening segment by inducing two DSBs into genomic DNA by employing CRISPR/Cas9 technology (40, 41) using synthesized gBlocks for sgRNA production. We knocked out the *PRDM1* gene and overexpressed PRDM1α and -β in RKO colon cancer cells and found that PRDM1 can repress the expression of stem cell-related genes. Overexpressing PRDM1α and PRDM1β in RKO cells showed similar effects on gene regulation. Since PRDM1 is described as a repressor in B and T cells, the up-regulated 925 genes might be regulated by PRDM1 indirectly. Interestingly, Jun family members such as JUN, JUNB, and JUND were up-regulated by PRDM1 (Fig. 3*C*). It is noteworthy that KDM5B expression levels were increased by PRDM1 overexpression, which could lead to H3K4me2 and H3K4me3 demethylation and gene repression through indirect mechanisms. PRDM1 can repress specific genes not only by recruiting diverse chromatin-modifying proteins, such as G9a, HDAC1, HDAC2, and the

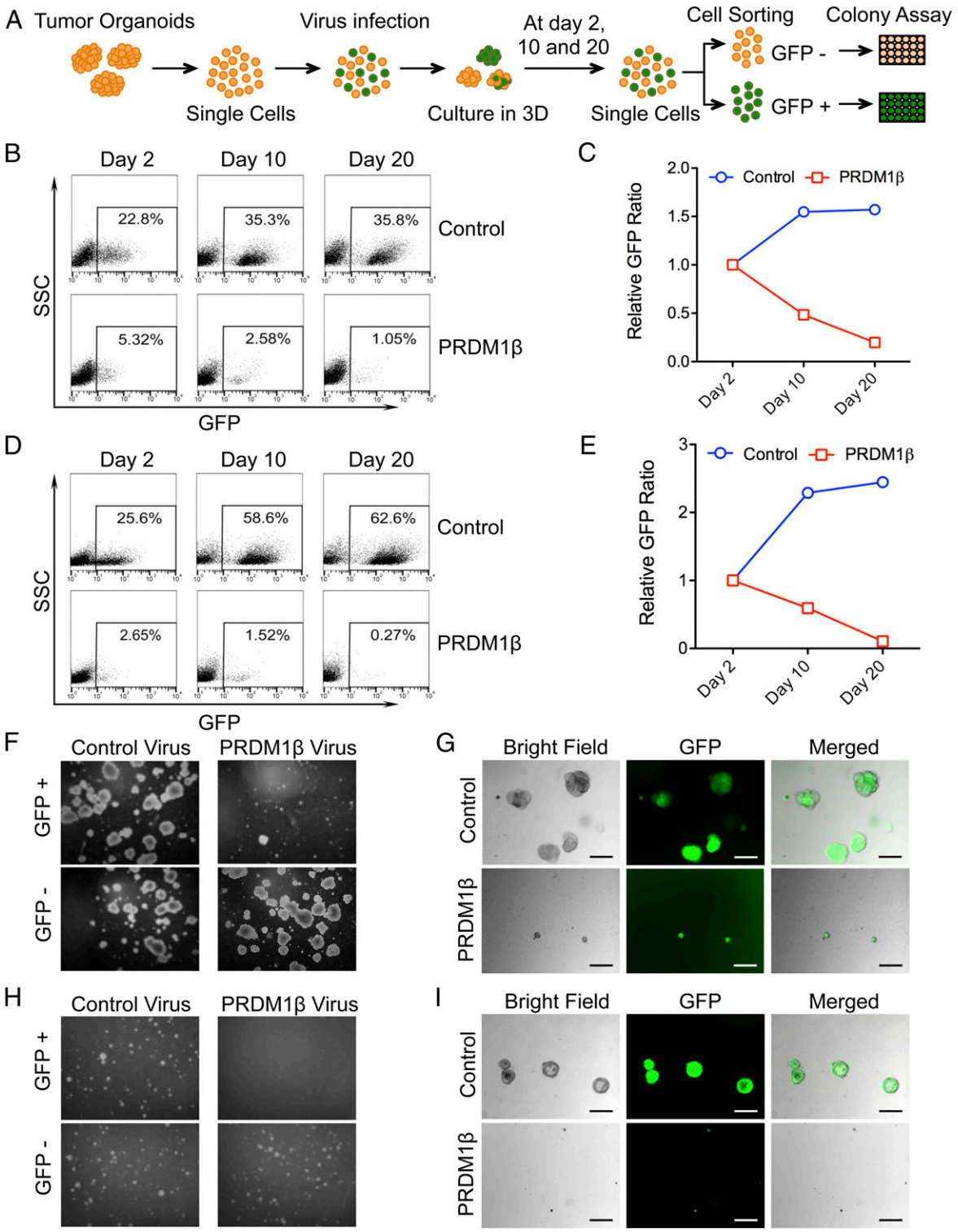

Fig. 5. PRDM1 inhibits colon tumor organoid clonal survival. (*A*) Schematic of the tumor organoid-forming assay. (*B*) Flow cytometry scatter plots showing the percentage of GFP^+ cells in P07132016 tumor organoids at the different time points indicated. (*C*) Percentages of GFP^+ cells were normalized to day 2 starting material. Relative GFP ratios from patient P07132016 are shown. (*D*) Flow cytometry scatter plots showing the percentage of GFP^+ cells in P10152015 tumor organoids at the indicated time points. (*E*) Percentages of GFP^+ cells were normalized to day 2 starting material. The relative GFP ratios from patient P10152015 are shown. (*F*) Representative images of the organoid-forming assay from patient P07132016 colon tumor organoids. GFP^+ cells and GFP^- cells from control or PRDM1-infected organoids were plated in Matrigel at a density of 500 cells per well in 24-well plates and were cultured for 14 d. Representative images are shown. (Magnification, 40×.) (*G*) Patient P07132016 organoids from control and PRDM1-infected cells were GPF^+. Organoids infected with control virus were larger and greater in number than those infected with PRDM1β virus. (*H*) Representative images of the organoid-forming assay from patient P10152015 colon tumor organoids. GFP^+ cells and GFP^- cells from control or PRDM1-infected organoids were plated in Matrigel at a density of 500 cells per well in 24-well plates and were cultured for 3–5 wk. Representative images are shown. (Magnification, 40×.) (*I*) Organoids derived from patient P10152016 infected with lentivirus containing PRDM1β and control virus are GPF^+. Organoids infected with control virus are larger and greater in number than those infected with PRDM1β virus. (Scale bars in *G* and *I*: 200 μm.)

transcriptional corepressor Groucho, generating regulatory complexes (19–21), but also by up-regulating demethylase genes such as *KDM5B*.

Two previous studies of the role of PRDM1 in cell proliferation in HCT116 and SW620 colon cancer cells draw different, contradictory conclusions (22, 25). PRDM1 loss of function in these studies was based on knockdown technology in which residual PRDM1 expression could still remain if PRDM1 is maintained at a low level in RKO cells (*SI Appendix*, Figs. S1*A* and S3 *D* and *E*). We used PRDM1-KO technology to completely abate *PRDM1* gene expression. Our study found that neither PRDM1-KO nor PRDM1 OE could affect RKO colon cancer cell proliferation significantly (*SI Appendix*, Fig. S5). The different results might be due to undescribed somatic mutations in these genetically unstable colon cancer cell lines.

It is now becoming clear that PRDM1 plays an important role as a tumor suppressor in B, T, and natural killer cell lymphomas (23, 42). In colorectal cancers, PRDM1β expression levels vary in primary tumors and are correlated with patient disease-free survival (Fig. 1*G*). Primary tumor cells that give rise to metastases often have molecular mechanisms and functional capabilities similar to those in normal stem cells. Previous studies show that breast cancers correlate with stem cell transcriptional signatures in the context of p53 inactivation (37). Our RNA-seq results indicated that PRDM1 inhibits the expression of genes that correlate with the stem cell transcriptional signature in RKO cells. Recently a long-term culture system has been developed that allows the in vitro expansion and study of normal and tumor epithelial cells from a variety of epithelial tissues. These cultures, referred to as "organoids," contain heterogeneous cell populations that derive from the normal stem cell compartment and reflect the in vivo cell-type diversity. We showed that p53 activation increased PRDM1β expression in normal colon organoids. Moreover, we adapted the culture conditions for the long-term expansion of colon tumor organoids and studied the effects of PRDM1β overexpression on colony-formation ability and stem cell expansion. The two organoids lines we used in this study are TP53-null organoids. These assays showed a strong negative selection pressure with progressive elimination of PRDM1-expressing cells. These findings are consistent with studies in natural killer cell lymphoma (23) and are likely due to PRDM1 silencing the cancer stem cell core gene network (Fig. 6*B*). Additionally, we found that PRDM1β is downstream of p53 protein in normal organoids, implying that p53 may eliminate abnormal epithelial stem cells through PRDM1 during cancer stem cell development by silencing stem cell genes. The mechanisms underlying the regulation of colon cancer stem cells and the possible effects on normal colon stem cell biology need to be addressed further.

In conclusion, our studies indicate that PRDM1β acts as a tumor-suppressor gene in colon tumor organoids, likely by acting downstream of p53. It modifies the expression of stem cell-related genes, inhibits colon epithelial cell proliferation, and is positively associated with good survival in colon cancer patients. Since PRDM1β exerts a role in human colon tumor organoids, it may be a viable target for therapeutic strategies aimed at reactivating the expression of PRDM1β in colon cancer cells.

Materials and Methods

Cell Culture. Human colon cancer RKO cells (kindly given by Bert Vogelstein, Sidney Kimmel Comprehensive Cancer Center at Johns Hopkins University, Baltimore) and its derivatives were maintained at 37 °C, 5% CO_2 in McCoy's 5A medium (Fisher) supplemented with 10% FBS, 100 U/mL penicillin, and 100 μg/mL streptomycin (Gibco). All cell lines were passaged in our laboratory for no more than 40 passages after resuscitation. Cells were passaged every 3–4 d to maintain subconfluence. Authentication of the RKO cell line was performed by Johns Hopkins University-Genetic Resources Core Facility Biorepository and Cell Center.

PRDM1 KO with CRISPR/Cas9. Human codon-optimized *Streptococcus pyogenes* wild-type Cas9 (Cas9-2A-GFP) was obtained from Addgene (no. 44719). Chimeric guide RNA expression cassettes with different sgRNAs (sgRNA1: AGCCGCACAGACGCGCACCT; sgRNA2: AAAACGTGTGGGTACGACCT; sgRNA3: CACAGGAACGGCGGGACAAT; sgRNA4: TGATGGCGGTACTTCGGTTC; sgRNA5: GCCATAACAAAGCGAACACT; sgRNA6: GTGTTACTTTAGGACTTGGA; sgRNA7: GCAGAAATCAGGGCGGAAAC; sgRNA8: AGGGGCAGAACCGACATTAC) were ordered as gBlocks. These gBlocks were amplified by PCR using the following primers: gBlock_Amplifying_F: 5′-GTACAAAAAAGCAGGCTTTAAAGG-3′ and gBlock_Amplifying_R: 5′-TAATGCCAACTTTGTACAAGAAAGC-3′. The PCR product was purified by Agencourt Ampure XP PCR Purification beads according to the manufacturer's protocol (Beckman Coulter). One microgram of Cas9 plasmid and 0.3 μg of each gRNA gBlock were cotransfected into RKO cells via Lipofectamine 3000. GFP^+ cells were collected by FACS 48 h after transfection. Cells were limiting diluted into 96-well plates. Cells were incubated at 37 °C in a CO_2 incubator for 2–3 wk for single-clone generating.

Library Construction and RNA-Seq. RNA was extracted from RKO derivatives using the miRNeasy Mini Kit (catalog no. 217004; Qiagen), and RNA-seq libraries were constructed using TruSeq Stranded mRNA LT (catalog no. RS-122-2101; Illumina) according to the manufacturers' protocols. The DNA libraries were qualified on an Agilent Technologies 2100 Bioanalyzer using an Agilent DNA 1000 chip and were quantitated by qPCR in a Bio-Rad iCycler using a Bio-Rad iCycler qPCR Master Mix (catalog no. KK4844; Kapa Biosystems). After denaturing, libraries were diluted to 1.8 pM with hybridization buffer. Paired-end 75-bp sequencing was performed on the Illumina NextSeq 500 benchtop sequencer using the NextSeq 500 High-output Kit v2 (150 CYS; catalog no. FC-404-2002; Illumina) per the manufacturer's protocol.

RNA-Seq Analysis. Sequencing reads were mapped to the human genome (hg19) using TopHat. Uniquely mapped reads were assembled into transcripts guided by the University of California, Santa Cruz (UCSC) *Homo sapiens* hg19 RefSeq and Gencode gene annotation. Expression differences between conditions were evaluated using DESeq2 (43, 44). Pearson's coefficient was calculated using the cor function with default parameters in R (https://www.r-project.org/). The hierarchical clustering analysis of the global gene-expression pattern in different samples was carried out using the heatmap.2 function (gplots package) in R. Gene set enrichment was analyzed with GSEA software (35). RNA-seq data have been deposited in the Gene Expression Omnibus (GEO) database (accession no. GSE101668).

Human Tissue Processing and Crypt Isolation. Colonic tissues were obtained from the University of Alabama at Birmingham Hospital with informed consent. All patients were diagnosed with colorectal cancer. From the resected colon segment, normal as well as tumor tissue was isolated. The isolation of normal crypts and tumor epithelium was performed as described (28–30, 45).

For normal colon crypts isolation, human colon tissues were cut into small pieces. These pieces were washed three times with ice-cold Dulbecco's PBS (DPBS) and then were incubated in cold DPBS supplemented with 2.5 mM EDTA for 40 min at 4 °C with gentle rotation. Then tubes were shaken vigorously to release crypts. The supernatant containing crypts was centrifuged. The crypts were subsequently washed twice with DPBS and resuspended in Matrigel with about 100–200 crypts per 50 μL of Matrigel. Fifty microliters of the crypt–Matrigel suspension were dispensed into the center of each well of a 37 °C prewarmed 24-well plate. The Matrigel was polymerized for 10 min at 37 °C. Human intestinal stem cell (HISC) medium was added, and the crypts were incubated at 37 °C, 5% CO_2 until they were ready to split. The composition of HISC medium was advanced DMEM/F12, 100 U/mL penicillin, 100 μg/mL streptomycin, 2 mM GlutaMAX, 10 mM Hepes, 1× N2, 1× B27 (Invitrogen), 1 mM *N*-acetyl-cysteine (Sigma), 10 mM Gastrin (Sigma) I, 50% Wnt-conditioned medium, 10% R-Spondin–conditioned medium, 100 ng noggin (Peprotech), 10 mM nicotinamide (Sigma), 50 ng/mL human EGF (Invitrogen), 500 nM A83-01 (Sigma), and 3 μM SB202190 (Sigma) (*SI Appendix*, Table S2).

For tumor epithelium isolation, tumor tissues were cut into small pieces and incubated in DPBS with collagenase/hyaluronidase (catalog no. 07919; STEMCELL Technology; final concentration: 2 mg/mL collagenase, 200 U/mL hyaluronidase) and 10 mM ROCK inhibitor for 30 min at 37 °C with shaking. After incubation, heat-inactivated FBS (5%) was added, and the mixture was allowed to sit for 2 min. Then the supernatant was transferred to a new tube to remove large fragments. Cells were subsequently spun at 350 × *g* for 3 min. The pellet was washed twice in DBPS to remove debris and collagenase. The tumor epithelium was resuspended in Matrigel and plated at

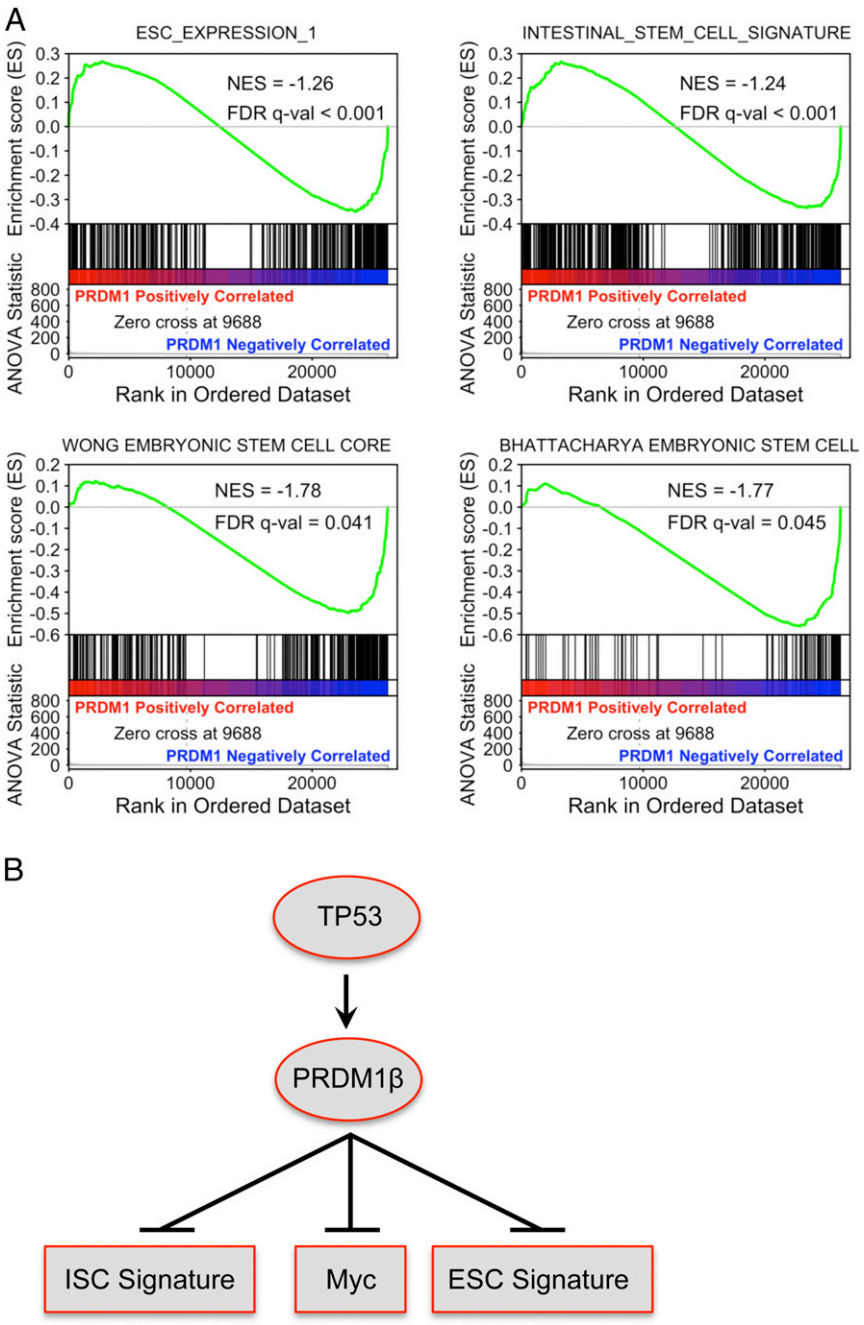

Fig. 6. PRDM1 results in the down-regulation of the embryonic stem cell signature in cancer cells and the intestinal stem cell signature in normal intestinal stem cells. (*A*) GSEA of the embryonic stem cell signature and intestinal stem cell signature. ESC_EXPRESSION_1 contains 380 genes from Ben-Porath et al. (38); INTESTINAL_STEM_CELL_SIGNATURE contains 511 genes from Merlos-Suárez et al. (39). (*B*) A model illustrating the regulation of colon cancer cell proliferation by PRDM1 via multiple genes.

different densities. After the Matrigel was allowed to solidify, HISC medium without Wnt3a was added, and the cells were incubated at 37 °C, 5% CO_2.

Organoid Culture. The tumor and normal colon organoid culture medium was refreshed every 2 d. To passage the organoids, Matrigel was broken up with medium using a 1-mL pipette tip and was transferred from the well to a 15-mL tube. The organoids were centrifuged at 400 × *g* for 4 min, and the medium was removed. One milliliter of TrypLE Selection (Invitrogen) was added, and the organoids were incubated at 37 °C for ∼5 min. Basal medium (Advanced DMEM/F12, 100 U/mL penicillin, 100 μg/mL streptomycin, 2 mM GlutaMAX, 10 mM Hepes) was added, and cells were spun down at 400 × *g* for 4 min. The pellet was resuspended in Matrigel, and cells were plated in droplets of 50 μL each in each well of 24-well plates. After the Matrigel was allowed to solidify, HISC medium (for normal organoids) or HISC medium minus Wnt (for tumor organoids), both supplemented with 10 μM ROCK inhibitor, was added to the plates, and organoids were incubated at 37 °C, 5% CO_2.

Tumor Organoid-Forming Assay.

Infection. The tumor organoids were cultured in 3D Matrigel culture. The Matrigel was disrupted by pipetting, and organoids were collected into a 15-mL tube. The organoids were centrifuged at 400 × *g* for 4 min, and the supernatant was removed. Five microliters of TrypLE Selection (Invitrogen) were added, and the organoids were incubated at 37 °C for 20–40 min. Every 5 min organoids were fractured by up-and-down pipetting with 1-mL tips. When most of the organoids were digested to single cells, basal medium (Advanced DMEM/F12, 2 mM GlutaMAX, 10 mM Hepes, 1× penicillin/streptomycin)

was added, and cells were spun down at 400 × *g* for 4 min. Cells were counted and resuspended in 500 μL of culture medium with 3 MOI of PRDM1β or control virus, 6 μg/mL Polybrene (Santa Cruz Biotechnology), and 10 μM ROCK inhibitor. Cells were transferred into one well of a 24-well plate and were incubated at 37 °C 5% CO_2. After 6 h incubation, cells were collected into a 1.5-mL tube and were centrifuged at 400 × *g* for 4 min. Cells were resuspended in Matrigel and were replated in 50-μL droplets in each well of 24-well plates.

Cell sorting and organoid formation. Cell sorting was done at days 2, 10, and 20 after virus transduction. Briefly, organoids were digested with TrypLE to single cells as described above. Both GFP^+ and GFP^- cells were collected by FACS. Five hundred single cells were resuspended in 50 μL of Matrigel and replated in one well of 24-well plates. These cells were cultured for 3–5 wk. The percentage of GFP^+ cells was determined during cell sorting.

PRDM1 KO in Human Colon Tumor Organoids. Lentiviral vectors for Cas9 (catalog no. TECC1002), PRDM1 sgRNA (catalog no. TEDH-1062730), and control sgRNA (catalog no. TELA1015) were purchased from transOMIC Technologies. Lentiviruses were packaged, concentrated, and titered. Tumor organoids were collected and digested with TrypLE to single cells. Cells were infected with 1 MOI of Cas9 virus and 1 MOI of PRDM1 sgRNA virus or control sgRNA virus. After infection, cells were cultured in Matrigel with tumor HISC medium with Blasticidin S and puromycin. The positive organoids were cultured and then were used for the organoid-forming assays.

Statistical Analysis. All data were analyzed with GraphPad Prism 6 (GraphPad Software) and are provided as mean ± SEM unless otherwise indicated. Statistical analyses were performed using an unpaired Student's *t* test. The significance level (*P* value) was set at $*P < 0.05$, $**P < 0.01$, and $***P < 0.001$.

ACKNOWLEDGMENTS. We thank Dr. Chang-uk Lim at the Microscopy and Flow Cytometry Core Facility of the College of Pharmacy at the University of South Carolina for cell sorting. This work was supported by NIH Grant U01 CA158428 (to P.J.B.).

1. Keller AD, Maniatis T (1991) Identification and characterization of a novel repressor of beta-interferon gene expression. *Genes Dev* 5:868–879.
2. Turner CA, Jr, Mack DH, Davis MM (1994) Blimp-1, a novel zinc finger-containing protein that can drive the maturation of B lymphocytes into immunoglobulin-secreting cells. *Cell* 77:297–306.
3. de Souza FS, et al. (1999) The zinc finger gene Xblimp1 controls anterior endomesodermal cell fate in Spemann's organizer. *EMBO J* 18:6062–6072.
4. Vincent SD, et al. (2005) The zinc finger transcriptional repressor Blimp1/Prdm1 is dispensable for early axis formation but is required for specification of primordial germ cells in the mouse. *Development* 132:1315–1325.
5. Ohinata Y, et al. (2005) Blimp1 is a critical determinant of the germ cell lineage in mice. *Nature* 436:207–213.
6. Horsley V, et al. (2006) Blimp1 defines a progenitor population that governs cellular input to the sebaceous gland. *Cell* 126:597–609.
7. Magnúsdóttir E, et al. (2007) Epidermal terminal differentiation depends on B lymphocyte-induced maturation protein-1. *Proc Natl Acad Sci USA* 104:14988–14993.
8. Shaffer AL, et al. (2002) Blimp-1 orchestrates plasma cell differentiation by extinguishing the mature B cell gene expression program. *Immunity* 17:51–62.
9. Lin Y, Wong K, Calame K (1997) Repression of c-myc transcription by Blimp-1, an inducer of terminal B cell differentiation. *Science* 276:596–599.
10. Sciammas R, Davis MM (2004) Modular nature of Blimp-1 in the regulation of gene expression during B cell maturation. *J Immunol* 172:5427–5440.
11. Martins GA, et al. (2006) Transcriptional repressor Blimp-1 regulates T cell homeostasis and function. *Nat Immunol* 7:457–465.
12. Kallies A, et al. (2006) Transcriptional repressor Blimp-1 is essential for T cell homeostasis and self-tolerance. *Nat Immunol* 7:466–474.
13. Gong D, Malek TR (2007) Cytokine-dependent Blimp-1 expression in activated T cells inhibits IL-2 production. *J Immunol* 178:242–252.
14. Martins GA, Cimmino L, Liao J, Magnusdottir E, Calame K (2008) Blimp-1 directly represses Il2 and the Il2 activator Fos, attenuating T cell proliferation and survival. *J Exp Med* 205:1959–1965.
15. Lin IY, et al. (2014) Suppression of the SOX2 neural effector gene by PRDM1 promotes human germ cell fate in embryonic stem cells. *Stem Cell Reports* 2:189–204.
16. Nagamatsu G, Saito S, Takubo K, Suda T (2015) Integrative analysis of the acquisition of pluripotency in PGCs reveals the mutually exclusive roles of Blimp-1 and AKT signaling. *Stem Cell Reports* 5:111–124.
17. Tang WW, et al. (2015) A unique gene regulatory network resets the human germline epigenome for development. *Cell* 161:1453–1467.
18. Ancelin K, et al. (2006) Blimp1 associates with Prmt5 and directs histone arginine methylation in mouse germ cells. *Nat Cell Biol* 8:623–630.
19. Yu J, Angelin-Duclos C, Greenwood J, Liao J, Calame K (2000) Transcriptional repression by blimp-1 (PRDI-BF1) involves recruitment of histone deacetylase. *Mol Cell Biol* 20:2592–2603.
20. Gyory I, Wu J, Fejér G, Seto E, Wright KL (2004) PRDI-BF1 recruits the histone H3 methyltransferase G9a in transcriptional silencing. *Nat Immunol* 5:299–308.
21. Ren B, Chee KJ, Kim TH, Maniatis T (1999) PRDI-BF1/Blimp-1 repression is mediated by corepressors of the Groucho family of proteins. *Genes Dev* 13:125–137.
22. Yan J, et al. (2007) BLIMP1 regulates cell growth through repression of p53 transcription. *Proc Natl Acad Sci USA* 104:1841–1846.
23. Küçük C, et al. (2011) PRDM1 is a tumor suppressor gene in natural killer cell malignancies. *Proc Natl Acad Sci USA* 108:20119–20124.
24. Weige CC, et al. (2014) Transcriptomes and shRNA suppressors in a TP53 allele-specific model of early-onset colon cancer in African Americans. *Mol Cancer Res* 12:1029–1041.
25. Kang HB, et al. (2016) PRDM1, a tumor-suppressor gene, is induced by genkwadaphnin in human colon cancer SW620 cells. *J Cell Biochem* 117:172–179.
26. György I, Fejér G, Ghosh N, Seto E, Wright KL (2003) Identification of a functionally impaired positive regulatory domain I binding factor 1 transcription repressor in myeloma cell lines. *J Immunol* 170:3125–3133.
27. Relógio A, et al. (2014) Ras-mediated deregulation of the circadian clock in cancer. *PLoS Genet* 10:e1004338.
28. van de Wetering M, et al. (2015) Prospective derivation of a living organoid biobank of colorectal cancer patients. *Cell* 161:933–945.
29. Fujii M, Matano M, Nanki K, Sato T (2015) Efficient genetic engineering of human intestinal organoids using electroporation. *Nat Protoc* 10:1474–1485.
30. Sato T, et al. (2011) Long-term expansion of epithelial organoids from human colon, adenoma, adenocarcinoma, and Barrett's epithelium. *Gastroenterology* 141:1762–1772.
31. Huang B, Deo D, Xia M, Vassilev LT (2009) Pharmacologic p53 activation blocks cell cycle progression but fails to induce senescence in epithelial cancer cells. *Mol Cancer Res* 7:1497–1509.
32. Ho TT, et al. (2015) Targeting non-coding RNAs with the CRISPR/Cas9 system in human cell lines. *Nucleic Acids Res* 43:e17.
33. Canver MC, et al. (2014) Characterization of genomic deletion efficiency mediated by clustered regularly interspaced short palindromic repeats (CRISPR)/Cas9 nuclease system in mammalian cells. *J Biol Chem* 289:21312–21324.
34. Ding Q, et al. (2013) Enhanced efficiency of human pluripotent stem cell genome editing through replacing TALENs with CRISPRs. *Cell Stem Cell* 12:393–394.
35. Subramanian A, et al. (2005) Gene set enrichment analysis: A knowledge-based approach for interpreting genome-wide expression profiles. *Proc Natl Acad Sci USA* 102:15545–15550.
36. Doody GM, et al. (2010) An extended set of PRDM1/BLIMP1 target genes links binding motif type to dynamic repression. *Nucleic Acids Res* 38:5336–5350.
37. Mizuno H, Spike BT, Wahl GM, Levine AJ (2010) Inactivation of p53 in breast cancers correlates with stem cell transcriptional signatures. *Proc Natl Acad Sci USA* 107:22745–22750.
38. Ben-Porath I, et al. (2008) An embryonic stem cell-like gene expression signature in poorly differentiated aggressive human tumors. *Nat Genet* 40:499–507.
39. Merlos-Suárez A, et al. (2011) The intestinal stem cell signature identifies colorectal cancer stem cells and predicts disease relapse. *Cell Stem Cell* 8:511–524.
40. Cong L, et al. (2013) Multiplex genome engineering using CRISPR/Cas systems. *Science* 339:819–823.
41. Jinek M, et al. (2012) A programmable dual-RNA-guided DNA endonuclease in adaptive bacterial immunity. *Science* 337:816–821.
42. Boi M, Zucca E, Inghirami G, Bertoni F (2015) PRDM1/BLIMP1: A tumor suppressor gene in B and T cell lymphomas. *Leuk Lymphoma* 56:1223–1228.
43. Love MI, Huber W, Anders S (2014) Moderated estimation of fold change and dispersion for RNA-seq data with DESeq2. *Genome Biol* 15:550.
44. Schurch NJ, et al. (2016) How many biological replicates are needed in an RNA-seq experiment and which differential expression tool should you use? *RNA* 22:839–851.
45. Weeber F, et al. (2015) Preserved genetic diversity in organoids cultured from biopsies of human colorectal cancer metastases. *Proc Natl Acad Sci USA* 112:13308–13311.